

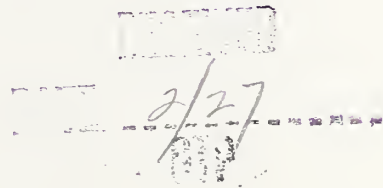
Today - 313.05 - 200



NBSIR 75-952

An Error Analysis of Failure Prediction Techniques Derived From Fracture Mechanics

S. M. Wiederhorn, E. R. Fuller, Jr., J. Mandel, and A. G. Evans*



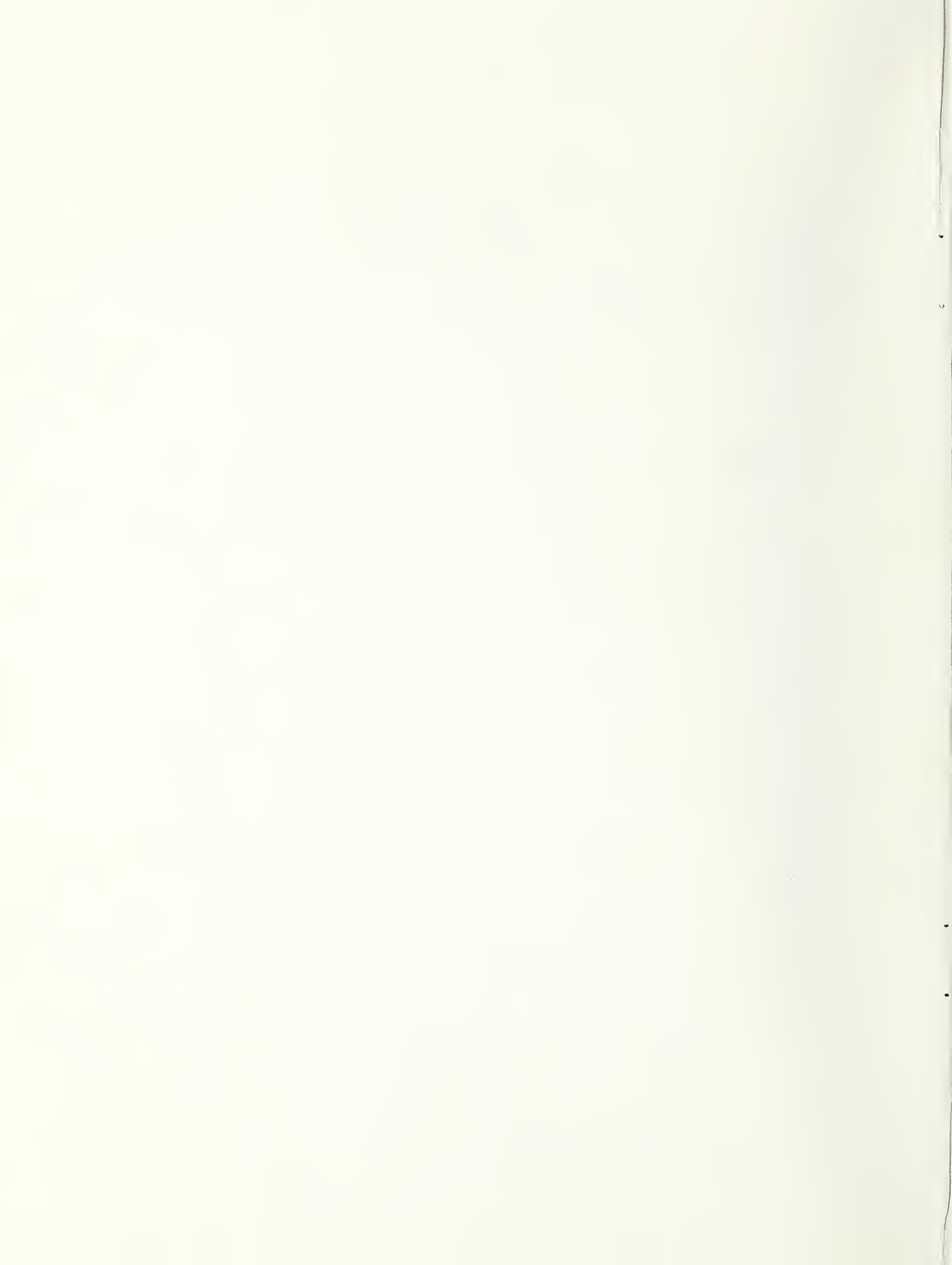
Inorganic Materials Division
Institute for Materials Research
National Bureau of Standards
Washington, D. C. 20234

*Science Center, Rockwell International
Thousand Oaks, California 91360

December 1975

Interim Report for Period July 1, 1975 through December 30, 1975

Prepared for
**Department of the Air Force
Materials Research Laboratory
Wright Patterson Air Force Base
Dayton, Ohio**



NBSIR 75-952

AN ERROR ANALYSIS OF FAILURE PREDICTION TECHNIQUES DERIVED FROM FRACTURE MECHANICS

S. M. Wiederhorn, E. R. Fuller, Jr., J. Mandel, and A. G. Evans*

Inorganic Materials Division
Institute for Materials Research
National Bureau of Standards
Washington, D. C. 20234

*Science Center, Rockwell International
Thousand Oaks, California 91360

December 1975

Interim Report for Period July 1, 1975 through December 30, 1975

Prepared for
Department of the Air Force
Materials Research Laboratory
Wright Patterson Air Force Base
Dayton, Ohio



U.S. DEPARTMENT OF COMMERCE, Rogers C.B. Morton, *Secretary*
James A. Baker, III, *Under Secretary*
Dr. Betsy Ancker-Johnson, *Assistant Secretary for Science and Technology*
NATIONAL BUREAU OF STANDARDS, Ernest Ambler, *Acting Director*

ABSTRACT

Three principal methods of failure prediction for brittle materials are analyzed statistically. Each method depends on fracture mechanics for its predictive value and hence, the variance of the failure time is found to depend on the scatter in the fracture mechanics data and the scatter in the estimate of the initial size of the strength limiting crack. The variance is used to calculate confidence limits for the prediction of failure for two materials, glass and silicon carbide. Procedures for the collection and analysis of data are discussed, and the implications of the analysis for lifetime prediction are evaluated.

1. INTRODUCTION

Recent developments in the application of fracture mechanics to brittle materials have provided improved design methods to assure structural reliability.¹⁻³ Since brittle materials generally fail from preexisting cracks, these design methods are based on a characterization of crack size and subcritical crack growth. Crack growth data obtained by fracture mechanics techniques are used to construct design diagrams, from which predictions of lifetime can be made for a given set of service conditions. Three types of diagrams have been developed. Each depends on a different technique to estimate the size of the crack that causes failure. One method requires direct measurement of the crack size by nondestructive techniques. A second method uses proof testing to eliminate specimens with cracks greater than a given maximum size. The third method uses strength measurements to obtain a statistical description of the crack size distribution in the body. Once the crack size has been determined, the time to failure and the strength can be estimated from the fracture mechanics data.

The accuracy of lifetime predictions depends on the accuracy with which the crack growth data and the initial crack size can be determined.⁴ Both of these are experimental quantities, and as such are influenced by errors of measurement. Both systematic and random errors are important. Errors of measurement result in uncertainties in predicting the lifetime and strength of structural components. Since it is not possible to completely eliminate errors of measurement, an error analysis is needed to establish confidence limits for the application of fracture mechanics to structural design. The purpose of this paper is to provide just such an analysis.

The uncertainty in the failure time is estimated from the variance (of both the fracture mechanics data and the flaw size detection capability), using standard statistical techniques. Then, for illustration purposes, confidence limits are determined using fracture mechanics and strength data for two brittle materials, glass and silicon carbide. Finally, the practical implications of the analysis for data collection and for lifetime prediction are discussed.

2. THEORY

2.1 Variance of Time to Failure

Fracture mechanics techniques have been used to collect crack growth data on a variety of brittle materials. In general, it has been shown that the quasi-static crack velocity, v , can be expressed as a power function of the stress intensity factor, K_I^* ,

$$v = v_0 (K_I / K_0)^n \quad (1)$$

where v_0 and n are empirical constants determined by a least squares fit of crack growth data; K_0 is the value of K_I which is selected to express the stress intensity

*A similar expression pertains to fatigue crack propagation, $da/dN \propto (\Delta K)^n$, and a statistical analysis, which is equivalent to that presented here for quasistatic crack propagation, can be applied to fatigue data.

factor in dimensionless form. K_0 has often been assigned the (arbitrary) value $1 \text{ Nm}^{-3/2}$.

As shown by the following equation,^{5,6} the time to failure, t , depends on the applied stress, σ_a , the crack velocity, v , the critical stress intensity factor, K_{Ic} , and the stress intensity factor, K_{Ii} , at the most serious crack when it is first subjected to a load:

$$t = (2/\sigma_a^2 Y^2) \int_{K_{Ii}}^{K_{Ic}} (K_I/v) dK_I \quad (2)$$

where Y is a constant that depends on flaw and specimen geometry and relates the applied stress and flaw size to the stress intensity factor ($K_I = \sigma_a Y \sqrt{a}$).

By substituting equation (1) into equation (2), t can be expressed in closed form. For $n \gtrsim 10$, t is given, to a good approximation, by the following equation:

$$t = (2 K_0^n / (n-2) Y^2 v_0 \sigma_a^2) K_{Ii}^{-(n-2)} \quad (3)$$

The error analysis is performed more easily if equation (3) is expressed in logarithmic form; then $\ln t$ has the following functional relationship to experimental and design variables:

$$\ln t = f(n, \ln v_0, \ln K_{Ii}, \ln \sigma_a) \quad (4)$$

Using error propagation theory* the variance of $\ln t$ is given by the following equation:⁷

$$\begin{aligned} V(\ln t) = & (\partial f / \partial n)^2 V(n) + 2(\partial f / \partial n)(\partial f / \partial \ln v_0) \text{Cov}(n, \ln v_0) \\ & + (\partial f / \partial \ln v_0)^2 V(\ln v_0) + (\partial f / \partial \ln K_{Ii})^2 V(\ln K_{Ii}) \\ & + (\partial f / \partial \ln \sigma_a)^2 V(\ln \sigma_a) + 2(\partial f / \partial \ln K_{Ii})(\partial f / \partial \ln \sigma_a) \text{Cov}(\ln K_{Ii}, \ln \sigma_a) \quad (5) \end{aligned}$$

* Since f is a non-linear function, a linearized error propagation theory for the error in $\ln t$ has been used. This linearization is valid when the relative errors in n and $\ln K_{Ii}$ are of the order of 10% or smaller.⁷ The validity of this approach is supported by recent unpublished work by Ritter and Jacobs who show that $V(\ln t)$ obtained by a Monte Carlo method is in substantial agreement with that obtained in this paper.

The first three terms to the right of the equality represent the contribution to $V(\ln t)$ from uncertainties in the crack propagation data. A covariance term is included because n and $\ln v_0$ are not statistically independent quantities. This term is needed to eliminate any dependence of $V(\ln t)$ on the set of axes selected to represent the crack propagation data. The fourth term to the right of the equality represents uncertainties in the value of $\ln K_{Ij}$, while the fifth term represents uncertainties in $\ln \sigma_a$. The sixth term accounts for possible statistical interdependence between $\ln K_{Ij}$ and $\ln \sigma_a$.

Substituting equations (3) and (4) into (5) we obtain;

$$V(\ln t) = [\ln K_{Ij} - \ln K_0 + (n-2)^{-1}]^2 V(n) + 2[\ln K_{Ij} - \ln K_0 + (n-2)^{-1}] \text{Cov}(n, \ln v_0) \\ + V(\ln v_0) + (n-2)^2 V(\ln K_{Ij}) + 4 V(\ln \sigma_a) + 4(n-2) \text{Cov}(\ln K_{Ij}, \ln \sigma_a) \quad (6)$$

The variance terms of equation (6) can be evaluated from the crack propagation data and from an analysis of the method used to determine $\ln K_{Ij}$. $\ln \sigma_a$ is a design variable that is assumed to have a known value for purposes of this paper (i.e. $V(\ln \sigma_a) = 0$ and $\text{Cov}(\ln K_{Ij}, \ln \sigma_a) = 0$). In a real component, these variances are not zero, and their values depend on how close the design stresses approximate those actually present in a component.

2.2 Variance From Crack Propagation Parameters

The parameters in the crack propagation terms of equation (6) are determined by the classical method of least squares. The fit of the crack propagation data is performed $\ln K_I$ upon $\ln v$ (see Appendix A);

$$\ln K_I = (\ln K_0 - \frac{1}{n} \ln v_0) + \frac{1}{n} \ln v, \quad (7)$$

where n and $\ln v_0$ are given by,

$$1/n = \left[\sum_{j=1}^N (\ln K_{Ij} - \langle \ln K_I \rangle) (\ln v_j - \langle \ln v \rangle) \right] / \left[\sum_{j=1}^N (\ln v_j - \langle \ln v \rangle)^2 \right] \quad (8)$$

$$\ln v_0 = \langle \ln v \rangle - n (\langle \ln K_I \rangle - \ln K_0) \quad (9)$$

where $\langle \ln v \rangle = (\sum_{j=1}^N \ln v_j)/N$; $\langle \ln K_I \rangle = (\sum_{j=1}^N \ln K_{Ij})/N$ and N is the total number of data points.

$V(n)$ and $V(\ln v_0)$ are given by the following equations:

$$V(n) = n^4 V(\delta) / \sum_{j=1}^N (\ln v_j - \langle \ln v \rangle)^2 \quad (10)$$

$$V(\ln v_0) = (\langle \ln K_I \rangle - \ln K_0)^2 V(n) + n^2 V(\delta)/N \quad (11)$$

where

$$V(\delta) = \left[\sum_{j=1}^N (\ln K_{Ij} - \ln K_0 + \frac{1}{n} \ln v_0 - \frac{1}{n} \ln v_j)^2 \right] / (N-2) \quad (12)$$

Finally, $\text{Cov}(n, \ln v_0)$ is obtained by methods given in Appendix B:

$$\text{Cov}(n, \ln v_0) = -(\langle \ln K_I \rangle - \ln K_0) V(n) \quad (13)$$

Substitution equations 11 and 13 into equation 6, $V(\ln t)$ reduces to:

$$\begin{aligned} V(\ln t) = & [\ln K_{Ii} - \langle \ln K_I \rangle + (n-2)^{-1}]^2 V(n) + n^2 V(\delta)/N \\ & + (n-2)^2 V(\ln K_{Ii}) \end{aligned} \quad (14)$$

Note that $V(\ln t)$ does not depend on K_0^* . Thus, the error in the time-to-failure prediction does not depend on the set of axes, or the system of units, which are used to represent the crack propagation data. As noted above, this result can be attributed to the covariance term in equation (5).

The above result (equation 14) can be used only if the errors of measurement are random, i.e. the data points must be statistically independent. In crack growth studies statistical independence is usually obtained when each data point is determined on a separate specimen. Then, errors resulting from indeterminate characteristics of specimens are limited to only a single data

*Although $V(\delta)$, as given by equation 12, appears to depend on K_0 , substitution of equation 9 into 12 shows that the variance of the fit $V(\delta)$ is independent of K_0 .

point. The errors do not propagate through an entire set of data as they would if an entire K_I - v curve was generated from a single specimen. Systematic shifts of crack propagation data that have been reported in the literature are due to the fact that complete sets of crack propagation data were collected from individual specimens^{4,8}. When statistically significant shifts occur between sets of K_I - v data, equation (14) is no longer applicable and other means of estimating $V(\ln t)$ must be found.* One method of analyzing sets of K_I - v data is to calculate the slope and intercept for each data set, and treat these slope-intercept pairs as estimates of the true slope and intercept, statistically independent from set to set. If n^α and $\ln v_0^\alpha$ are the slope and intercept obtained from equations (8) and (9) for the α^{th} set of crack propagation data and there are J such sets of data, then the mean values of the slopes and intercepts of the data are given by the following equations:⁺

$$\bar{n} = \left[\sum_{\alpha=1}^J n^\alpha \right] / J ; \quad \overline{\ln v_0} = \left[\sum_{\alpha=1}^J \ln v_0^\alpha \right] / J \quad (15)$$

and the variances of \bar{n} and $\overline{\ln v_0}$ are

$$V(\bar{n}) = \left[\sum_{\alpha=1}^J (n^\alpha - \bar{n})^2 \right] / (J-1) J \quad (16)$$

$$V(\overline{\ln v_0}) = \left[\sum_{\alpha=1}^J (\ln v_0^\alpha - \overline{\ln v_0})^2 \right] / (J-1) J \quad (17)$$

Finally, since \bar{n} and $\overline{\ln v_0}$ are not statistically independent parameters, the covariance of \bar{n} and $\overline{\ln v_0}$ are estimated from the following equation:

*However, if the shifts are not statistically significant (as determined by an analysis of variance^{7,9}), there may be justification for pooling the data, in which case equation (14) would be applicable.

+Note that the superscript α is an index and does not denote exponentiation.

$$\text{Cov}(\bar{n}, \overline{\ln v_0}) = \sum_{\alpha=1}^J (n^\alpha - \bar{n}) (\ln v_0^\alpha - \overline{\ln v_0}) / (J-1)J \quad (18)$$

An estimate of $V(\ln t)$ can now be obtained by substituting equations (15) through (18) into equation (6) (after using the transformation $n \rightarrow \bar{n}$ and $\ln v_0 \rightarrow \overline{\ln v_0}$). The equation obtained by this substitution is independent of K_0 , again demonstrating that the error in the predicted time to failure does not depend on the set of axes chosen to represent the crack propagation data.*

2.3 Variance From Initial Stress Intensity Factor

2.3.1. Direct Measurement

The initial stress intensity factor, K_{Ii} , can be determined by direct measurement of the initial crack length, a_i , which is then substituted into $K_{Ii} = \sigma_a Y \sqrt{a_i}$. The accuracy of K_{Ii} then depends on the accuracy of the crack length measurement;

$$V(\ln K_{Ii}) = (1/4) V(\ln a_i) \quad (19)$$

For a small relative error in the crack length measurement equation (19) becomes;

$$V(\ln K_{Ii}) = V(a_i) / 4a_i^2 \quad (19a)$$

where $V(a_i)$ is obtained by performing several completely independent flaw size determinations for each supercritical flaw (each scan contributes a single flaw size measurement, per flaw).

* Since the equation obtained by this substitution is more complex than equation 6, it is simpler to use equation 6 directly for an estimate of $V(\ln t)$.

2.3.2. Proof Testing

From fracture mechanics considerations it has been shown that the initial stress intensity factor, K_{Ii} , is related to the proof test stress, σ_p , by the following equation³:

$$K_{Ii} \leq K_{IC} (\sigma_p/\sigma_a)^{-1} \quad (20)$$

An estimate of the minimum time to failure, t_{min} , can be obtained by substituting relationship (20) into (3) and by using the equality sign of the relationship. $V(\ln K_{Ii})$ is now determined by the accuracy of the proof test ratio, σ_p/σ_a , and of the critical stress intensity factor:

$$V(\ln K_{Ii}) = V(\ln K_{IC}) + V(\ln \sigma_p/\sigma_a) \quad (21)$$

If the errors of these quantities are small then the following approximation is appropriate:

$$V(\ln K_{Ii}) = V(K_{IC})/K_{IC}^2 + (\sigma_p/\sigma_a)^{-2} V(\sigma_p/\sigma_a) \quad (22)$$

2.3.3. Strength Measurements

Strength measurements can be used to provide a statistical value of K_{Ii} . The strength in the absence of slow crack growth, σ_{IC} , is first determined on a series of ceramic components. The strength can then be related to the cumulative failure probability, P , by the use of order statistics.⁷ If the strength data fits a Weibull type distribution,¹⁰ then,

$$\ln Q \equiv \ln\{\ln [1/(1-P)]\} = m \ln(\sigma_{IC}/\sigma_o) \quad (23)$$

where σ_o and m are empirical constants determined from the data, and Q is defined as $\ln[1/(1-P)]$. A least squares fit of $\ln Q$ upon $\ln \sigma_{IC}$ can be used to determine m and σ_o .

By substituting $K_{Ic} = \sigma_{Ic} Y\sqrt{a_i}$ and $K_{Ii} = \sigma_a Y\sqrt{a_i}$ into equation (23), the following equation is obtained for K_{Ii} :

$$K_{Ii} = (\sigma_a/\sigma_o) K_{Ic} Q^{-1/m} \quad (24)$$

$V(\ln K_{Ii})$ is now given by the following expression:

$$\begin{aligned} V(\ln K_{Ii}) &= V(\ln \sigma_o) + \frac{1}{m^4} (\ln Q)^2 V(m) \\ &\quad - \frac{2}{m^2} (\ln Q) \text{Cov}(m, \ln \sigma_o) + V(\ln K_{Ic}) \end{aligned} \quad (25)$$

The covariance term is introduced into equation (25) because σ_o and m are not statistically independent. m and σ_o may be evaluated by the method of least squares.*

$$m = \frac{\sum_{r=1}^M [\ln Q_r] [\ln \sigma_r - \langle \ln \sigma \rangle]}{\sum_{r=1}^M (\ln \sigma_r - \langle \ln \sigma \rangle)^2} \quad (26)$$

$$\ln \sigma_o = \langle \ln \sigma \rangle - \frac{1}{m} \langle \ln Q \rangle \quad (27)$$

where

$$\langle \ln \sigma \rangle = \left(\sum_{r=1}^M \ln \sigma_r \right) / M \quad (28)$$

$$\langle \ln Q \rangle = \sum_{r=1}^M \ln Q_r / M \quad (29)$$

and M is the total number of strength measurements. The cumulative failure probability is given from order statistics as $P_r = r/(1+M)$ so that

$$Q_r = \ln [1/(1-P_r)].$$

*The subscript Ic has been dropped in these equations and a running subscript, r , has been used for the summations.

$V(m)$ and $V(\ln\sigma_0)$ are also obtained by the method of least squares

$$V(m) = V(\epsilon) / \sum_{r=1}^M (\ln\sigma_r - \langle \ln\sigma \rangle)^2 \quad (30)$$

$$V(\ln\sigma_0) = [\langle \ln Q \rangle]^2 V(m)/m^4 + V(\epsilon)/m^2 M \quad (31)$$

where $V(\epsilon)$ is the standard deviation of the fit given by the following equation

$$V(\epsilon) = \sum_{r=1}^M [\ln Q_r - m \ln(\sigma_r/\sigma_0)]^2 / (M-2) \quad (32)$$

The covariance of m and $\ln\sigma_0$ is derived in Appendix B :

$$\text{Cov}(m, \ln\sigma_0) = \langle \ln Q \rangle V(m)/m^2 \quad (33)$$

By substituting equations (31) and (33) into equation (25) the following expression is obtained for $V(\ln K_{Ii})$;

$$V(\ln K_{Ii}) = [\ln Q - \langle \ln Q \rangle]^2 V(m)/m^4 + V(\epsilon)/m^2 M + V(\ln K_{Ic}) \quad (34)$$

2.4 Estimation of Confidence Limits:

Once $V(\ln t)$ has been obtained, confidence limits are calculated from $V(\ln t)$ and a Student's t_a table*. To find t_a from the table, the number of

* t_a is not the time to failure, but is a number obtained from a Student's Statistical Table.

degrees of freedom, ν , has to be estimated from the experimental data. A method of estimating ν is given by Welch,¹¹ who discusses "Student's" problems when several different population variances are involved. For the direct flaw detection method ν is calculated from;

$$1/\nu = (1/\nu_v) [V(v)/V(\xi nt)]^2 + (1/\nu_a) \left[\frac{(n-2)}{2a_i} \right]^4 [V(a_i)/V(\xi nt)]^2 \quad (35)$$

where ν_v and ν_a are the number of degrees of freedom determined from the crack velocity and flaw size data respectively, and $V(v)$ is the component of $V(\xi nt)$ due to the crack propagation data [the first three terms in equation (6)]; ν_v is given simply by $N-2$ (where N is the number of velocity measurements*), and ν_a is given by the number of flaw-size measurements minus one.

For the proof test method;

$$1/\nu = (1/\nu_v) [V(v)/V(\xi nt)]^2 + (1/\nu_K) [V(K)/V(\xi nt)]^2 \quad (36)$$

where ν_K is the number of degrees of freedom determined from the critical stress intensity factor data, (equal to the number of K_{IC} tests minus one), and $V(K)$ is the component of $V(\xi nt)$ due to the critical stress intensity factor data [$V(K) = (n-2)^2 V(\xi n K_{IC})$].

The number of degrees of freedom for the strength method is given by;

$$1/\nu = (1/\nu_v) [V(v)/V(\xi nt)]^2 + (1/\nu_K) [V(K)/V(\xi nt)]^2 + (1/\nu_\sigma) [V(\sigma)/V(\xi nt)]^2 \quad (37)$$

where $V(\sigma)$ is the component of $V(\xi nt)$ resulting from the Weibull fit of the strength data [$(n-2)^2$ times the first two terms of Equation (34)] and ν_σ are the number of degrees of freedom ($M-2$) associated

* If equations (15-18) are used to estimate $V(v)$, ν_v is given by $J-1$ where J is the number of sets of $K-v$ data used to determine $V(v)$.

with that fit.

Once v has been estimated, t_a can be obtained and confidence limits for $\lambda n t$ can be calculated from the usual expression, $\pm t_a [V(\lambda n t)]^{1/2}$. The limits can be plotted on design diagrams to give an estimate of the uncertainty of the predicted failure time.

3. APPLICATION

3.1 Data Analysis and Collection

In this section, the theory presented in Section 2 is applied to two sets of experimental data; one set was collected on a low expansion silica glass (7.5 w% TiO_2 , 92.5 w% SiO_2);¹² the other set was collected on hot-pressed silicon carbide.¹³ The K-v curves determined from these data are shown in Fig. 1.

The glass data were collected in water using the double cantilever beam technique. Although there appears to be little scatter between the three curves, an analysis of variance shows⁹ them to be separate. Therefore, the between specimen scatter is significantly greater than the within specimen scatter, and $V(n)$, $V(\lambda n v_0)$ and $Cov(n, \lambda n v_0)$ have to be calculated from equations (15) through (18). $V(\lambda n t)$ is determined by using equation (6). Data on the strength (Fig. 2a) and critical stress intensity factor are also available for this glass, so that $V(\lambda n K_{Ij})$ can be estimated by the proof testing method, equation (21), and by the strength method, equation (34). An estimate of the initial flaw size ($\sim 10 \mu m$) can be obtained from the strength data. Since the small size of the strength impairing flaws in the glass precludes the use of non-destructive detection with presently available techniques, the variance calculations are not performed for this method.

The silicon carbide data were collected at high temperature (1400°C) using the double torsion technique. Since seven specimens were used to collect the data, equation (14) is appropriate for calculating $V(\lambda n t)$. Data for the

strength (Fig. 2b) and K_{IC} are also available and variance calculations can be performed for both the proof testing and strength methods. Again the small size of the initial flaws ($\sim 100\mu\text{m}$) precludes the use of non-destructive detection techniques to estimate initial flaw sizes.

The pertinent statistical data for the estimation of $V(\ln t)$ are listed in Tables 1 and 2; and the failure diagrams, including the 90% confidence limits, are presented in Figs. 3-7. For discussion purposes, the failure prediction methods are considered separately.

3.1.1 Direct Flaw Detection Method

The direct flaw detection approach is presently less definitive than the other two methods because the available test techniques have not been well quantified. Consequently, meaningful data which we can use to obtain $V(a_i)$ are simply not available. For completeness, however, we have indicated qualitatively in Fig. 3 the type of information we would anticipate from a flaw size determination based on the proviso that all flaws have been detected (this topic is discussed in more detail in Section 3.2.2). There will be a lower size limit of detection determined by the background scattering of the material, the test technique, and the relative physical properties*, of the defect and the material. For ceramic materials this lower limit is presently of the order of $100\mu\text{m}$, and this limit is indicated on the failure diagram (Fig. 3). Also, as the flaw size increases, the consistency of detection generally (but not always) improves; this will be reflected in a reduced $V(a_i)$ in equation 19.

3.1.2 Proof-Test Method

In the proof-test method the confidence limits depend on errors in both the crack propagation and critical stress intensity factor data. Since $V(\ln t)$ depends on $\ln K_{Ii}$, increasing as $\ln K_{Ii}$ decreases (see equation 14), the width of the confidence bands are expected to increase as the proof test ratio is

* For example, the ratio of acoustic impedances determines the intensity of the reflected and refracted waves for the commonly used ultrasonic techniques

increased. This increase in width is observed in both the glass and the silicon carbide diagrams (Fig. 4 and 5); it occurs because the lifetime calculations for large proof test ratios require extrapolation outside of the range of the crack propagation data. (This is discussed further in Section 3.2.2.) The broadening of the confidence limits is more apparent for silicon carbide than for the glass, reflecting a more accurate determination of K_{IC} for the silicon carbide. In fact the error in K_{IC} for glass was sufficiently large that it was the primary factor determining the width of the confidence interval.

The magnitude of the confidence band thus depends on both the basic material variability and the number of test specimens. It is not possible, therefore, to determine a priori the number of fracture mechanics tests and the (stress intensity factor) data range needed to achieve an acceptable separation of the confidence limits. These quantities must be re-established for each material. However, the silicon carbide exhibits a variability typical of ceramic polycrystals and we anticipate from the analysis of the silicon carbide data that about ten specimen will generally be sufficient for K_{IC} determinations and another ten for K, v determinations.*

3.1.3 Strength Method

Examination of the failure diagrams (Figs 6 and 7) for the strength method indicates that the width of the confidence band increases as the failure probability decreases, and the confidence bands broaden as the failure times increase.†

* For fused silica, for example, thirteen tests to determine K_{IC} gave a value of $(n-2)^2 V(\ln K_{IC})$ equal to 0.054; this compares with a value of 0.687 for four tests on the titania glass, described above.

† This effect is more apparent for the silicon carbide because the variance in K_{IC} is small compared to the other variance terms.

Again these effects occur because of the uncertainties that result from extrapolation of the strength and crack propagation data beyond the data limits.

Inspection of the individual variance terms indicates that the major contribution to the variance in the failure time emanates primarily from the variance in K_{IC} at high failure probabilities, but from the variance in the strength data at low failure probabilities. As discussed above, $V(\ln K_{IC})$ can be substantially reduced by obtaining a reasonable number of fracture mechanics data (about 10). We anticipate, therefore, that close control of the confidence band will generally be possible at the high probability extreme, with a modest test schedule. However, the variance in the strength data can only be significantly reduced at low probabilities by performing large numbers of tests. There are limits (of time and expense) to testing more than a few hundred specimens, and it thus becomes unreasonable to expect that a close separation of the confidence limits can be achieved at the low probability extreme. We suggest, therefore, that about twenty to forty strength tests be performed and that the resultant confidence limits should establish the lifetime expectancy for the material.

3.2 Life Prediction

For any well defined structural component, the service life, the stress distribution, the tolerable failure probability and the level of confidence should be clearly delineated quantities. The role of the lifetime prediction analysis is thus to identify test procedures which ensure that the component satisfies these structural specifications. The failure diagrams presented in Figs. 3-7 supply the pertinent information, at least in principle, and these can be used directly for a preliminary selection of a reliability test procedure. Certain limitations of the failure prediction methods should then be examined before embarking on a final selection.

3.2.1 Preliminary Test Method Selection

The preliminary selection process comprises the following steps. The failure diagrams are firstly developed for each test method from the fracture mechanics and strength data. The confidence bands, for the confidence level specified by the application, are then superimposed, as illustrated schematically in Fig. 8. The intersection of the specified lifetime and stress coordinates* on each diagram (Fig. 8) then designates the service requirements.

Commencing with the probability diagram (Fig. 8 a), the potential for utilizing the material without a nondestructive evaluation procedure can be assessed by comparing the location of the lower bound of the acceptable failure probability with the service condition. For the example in Fig. 8 a, the material would be acceptable for this application, without evaluation, if the tolerable failure probability were $\geq P_2$; but for failure probabilities $< P_2$, each component must be subjected to an evaluation procedure.

For materials which require evaluation, we now proceed to the proof test diagram (Fig. 8 b). The proof condition that ensures reliability is selected from the diagram by comparing the service condition with the lower confidence bound of the proof ratios. For the present example, (Fig. 8 b) the proof ratio, R_3 , would suffice.† Next by referring again to the probability diagram, the proportion of components that are likely to fail in the proof test can be estimated by determining the intersection of the stress coordinate at

* Hereafter termed the 'service condition'.

† The fact that the confidence band for each proof level extends over an order of magnitude (or more) in time is not an impediment to the application of the proof test technique, it simply requires that the proof ratio be set at a slightly larger value (see Figs. 4 and 5) than anticipated by the analysis that does not account for the data variability. The required increase in the proof test ratio, $\Delta\sigma_p/\sigma_a$, is given by: $\Delta\sigma_p/\sigma_a \approx (\sigma_p/\sigma_a) (t_a \sqrt{V(\ln t)})/(n-2)$; which can be derived from equations 3 and 20.

at the proof stress (σ_p), and the time coordinate for the time at the peak proof load (t_p) (Fig. 8 a). If this proportion is unacceptable (for economic reasons) the material is inadequate and an alternative material should be explored, this process should proceed until a material with a satisfactory proof test failure proportion is identified.

Finally, if proof testing is unsuitable (due, for example, to the complexity of the component), the direct flaw detection technique should be explored. The approach taken at this juncture is strongly material dependent. An approximate value for the flaw size that must be detected to ensure integrity is firstly obtained from the flaw size diagram, without accounting for the extension of the confidence limits (a_2 in Fig. 8c). Then the detectability of such flaw types should be evaluated using available NDE techniques. At this stage, confidence limits on flaw detection in the test material can be established for each NDE technique (the dotted lines in Fig. 8c), and the flaw size detection requirement can be more closely defined. The suitability of the material for this application is determined by the capability of detecting all flaws (in the critical parts of the component) that exceed the specified size.

3.2.2 Limitations

Each of the failure prediction approaches have limitations and these are briefly discussed here because they strongly influence the final selection of a test procedure. The prerequisites for effective proof testing have been discussed in detail in other publications³ and hence are only cursorily presented here for completeness. The proof test must be devised such that the stress in each element of the component exceeds the service stress in that same element by an amount at least as large as the recommended proof ratio. The

proof test must be performed under controlled conditions of environment and load cycle to validate the predicted lifetime. If these conditions can be satisfied, then proof testing is undoubtedly the best failure prediction method, because there are no unresolved aspects of the analysis and because the test errors are minimal.*

The strength method is unequivocal provided that the strength distribution function is determined on actual components (for each batch of material) under conditions that simulate the service condition. This requirement often poses an intolerable economic constraint, because large numbers of tests must be performed to achieve acceptable confidence. An alternative application of the strength method uses strength data obtained on small specimens machined randomly out of components selected from each batch. The specimen strength distribution is then converted into the appropriate component strength distribution using flaw size statistics. This approach is only valid if the flaw size statistics are treated correctly and if the flaw distribution function is invariant (i.e., the same for the components as for the specimen). Recent statistical treatments have established a basis for handling flaw size statistics correctly,¹⁴ but additional analytical developments (such as an allowance for the relative severity of internal and surface located flaws) are still required. Additionally, the validity of the constant flaw distribution assumption must be evaluated empirically for each material. Consequently, the strength method has minimal current application; but the specimen testing method may develop into a widely used approach if the uncertainties in the utility of the flaw size statistics are satisfactorily resolved.

The direct flaw detection method is the least definitive (for ceramic

* Each component is subjected to a single well-defined test, and the confidence band due to test error should then be insignificant.

materials), at its present stage of development. The two principal limitations are, the correctness of the predicted flaw size, and the requirement that all flaws larger than the specified size must be detected. A problem occurs with the prediction of the flaw size, because the microfracture mechanics parameters, that pertain to the extension of small preexisting flaws, can differ from the macrofracture mechanics parameters, obtained using conventional fracture mechanics specimens.* For certain materials, therefore, flaws smaller than the size predicted by the failure diagram may need to be detected.

The requirement that all supercritical flaws be detected can be a major source of test error. It is premature to attempt to ascertain the confidence limits due to test errors, but unless a highly automated test routine can be established, the confidence limits could be disturbingly expansive.

Finally, we discuss limitations in the analysis of lifetime prediction that originate from the limited range over which crack propagation data can be collected. If the initial stress intensity factor, K_{Ii} , is less than the minimum measured value of stress intensity factor, K_{Imin} , for the crack propagation data, it is necessary to extrapolate the crack propagation data beyond its range of measurement in order to obtain a lifetime prediction. The analysis of variance in Section 2.2 gives an estimate of the uncertainty involved in this extrapolation only if equation (1) is assumed to be valid for the region of extrapolation for which $K_{Ii} \leq K_I \leq K_{Imin}$. (A manifestation of this uncertainty is the broadening of the confidence limits which was noted

* The discrepancy between the micro- and macro- fracture mechanics parameters (when it occurs) generally appears as a difference in the absolute value of the stress intensity factor (i.e., in K_{Ic}) with no effect on the slope, n , and this only has a significant effect on failure prediction using the flaw size method.

in Section 3.1.2 for longer failure lifetimes.) However, since equation (1) is an empirical fit of crack propagation data, there is no a priori reason to expect such an extrapolation to provide an accurate prediction of failure lifetimes. In fact, other empirical equations sometimes fit the crack propagation data equally as well.⁶ For example, an exponential dependence of quasistatic crack velocity upon stress intensity factor, $v = v_1 \exp(b K_I/K_1)$, has been used to describe crack propagation data in glass and other ceramic materials. The power-function [equation (1)] and exponential-function representation of crack propagation data are compared in Figure 9, where $t_{\min} \sigma_a^2$ is plotted as a function of the proof-test ratio. The + in the figure marks the lower limit of the crack propagation data, for which $\sigma_p/\sigma_a = K_{Ic}/K_{Imin}$. The difference in lifetime prediction for larger proof-test ratios results from an extrapolation of the crack velocity data to values of K_I less than K_{Imin} . This diagram illustrates the importance of low-velocity data for effective failure predictions and the fact that extrapolation below this limit should be viewed with some caution. This limit can be easily incorporated in the failure diagrams. Substitution of the minimum measured stress intensity factor, K_{Imin} , into equation (3) for K_{Ij} , gives the maximum lifetime which can be predicted for a given applied stress without extrapolation of the crack propagation data. For the proof-test diagram, this is equivalent to a proof-test ratio of $\sigma_p/\sigma_a = K_{Ic}/K_{Imin}$. This same line applies to all three diagrams, as is illustrated schematically in Figure 10. Figure 10a also illustrates a region of extrapolation for the strength measurements to lower probabilities. Using order statistics, this limit is a probability of $P = 1/(M+1)$.

4. CONCLUSION

A method for the statistical treatment of data to be used for failure prediction has been presented. The analysis of two sets of typical data show that the 90% confidence bounds for the predicted lifetime can spread over two to four orders of magnitude (depending on the method used to estimate the initial flaw size). However, the stress allowables (or the conditions for the reliability test) based on the lower confidence bound do not differ substantially from those predicted from median values of the data, primarily because the slow crack growth exponents for ceramic materials are relatively large.

APPENDIX A

Least Square Fit of the Crack Propagation Data

The constants $\ln v_0$ and n (equation 1) are determined from a least squares fit of the crack propagation data. The method used to obtain this fit must give the best possible representation of the crack propagation data in order to obtain a reliable prediction of the time to failure. The classical method of applying a linear least squares fit to a set of data is based on the assumption that one of the variables of the fit (the independent variable) is free from error. The entire error of the fit is assumed to lie in the other variable (the dependent variable). Unfortunately, both variables of a least squares fit are often derived quantities and are subject to error. In the present analysis, both v and K_I are derived quantities and therefore are subject to error. v is often determined by direct measurement and its accuracy depends on the accuracy of measuring length and time. K_I is a calculated quantity that depends on measurements of specimen dimensions and crack length. In addition, other uncertainties such as crack tip shape and the orientation of the crack plane to the specimen surface can result in serious errors in measured K_I . Thus, for purposes of failure prediction it is necessary to demonstrate the applicability of the classical least squares method to the crack propagation data and to determine which variable (K_I or v) is to be assumed free from error.

An extensive discussion of the fitting of straight lines has been given by Mandel⁷. He has described a method of least squares that can be used when both variables are subject to error, provided independent estimates of the relative error in the two variables can be obtained. The method is somewhat more complicated than the classical method of least squares. Mandel has compared this more general method with the classical method and described the

conditions that must be met for the classical method to be applicable. For a linear equation $Y = \alpha + \beta X$, the parameter that must be considered to decide on the applicability of the classical method is the sensitivity ratio,

$$RS = \beta / (\sigma_y / \sigma_x) \quad (A1)$$

where σ_y and σ_x are independent estimates of the error in y and x respectively. If $RS \ll 1$ then the variables y and x should be fit y upon x (x is assumed to be free of error). However, if $RS \gg 1$ then the fit should be x upon y .

By applying these arguments to crack propagation data, it can be shown for most ceramic materials that K - v data should be fit $\ln K_I$ upon $\ln v$ ($\ln v$ is assumed to be free of error)*. In glass for example, $15 < \beta = n < 100$; $\sigma_{\ln v} \sim 0.03$; $\sigma_{\ln K} \sim 0.03$. Therefore, $RS = n / (\sigma_{\ln v} / \sigma_{\ln K}) > 15$, and the least square fit should be $\ln K$ upon $\ln v$. The constants of the least squares fit can then be calculated from the following equation,

$$\ln K_I = (\ln K_0 - \frac{1}{n} \ln v_0) + \frac{1}{n} \ln v \quad (A2)$$

which is just equation (1) rearranged.

* It should be emphasized that this conclusion may not be applicable for metals for which n is not a large quantity.

APPENDIX B

Estimate of the Covariance

The relationship between $\ln v_0$ and n is given by equation (9):

$$\ln v_0 = \langle \ln v \rangle - n(\langle \ln K_I \rangle - \ln K_0) \quad (B1)$$

From this equation we see that the intercept, $\ln v_0$, depends on the slope, n , the origin of the axis for measuring $\ln K_I$, $\ln K_0$, and the mean value of $\ln K_I$, $\langle \ln K_I \rangle$. Note that when $\langle \ln K_I \rangle = \ln K_0$, $\ln v_0 = \langle \ln v \rangle$. Thus, if the origin of $\ln K_I$ axis is selected to equal $\langle \ln K_I \rangle$, a regression analysis of $\ln K_I$ upon $\ln v$ yields a slope and intercept that are statistically independent. Using equation (B1) the regression analysis of $\ln K_I$ upon $\ln v$, equation (7), can be written as:

$$\ln K_I = \langle \ln K_I \rangle + \frac{1}{n} (\ln v - \langle \ln v \rangle) \quad (B2)$$

where $\langle \ln K_I \rangle$ is the intercept and $1/n$ is the slope of the fit. As already noted $\langle \ln K_I \rangle$ and $1/n$ are statistically independent. Therefore, $\text{Cov}(n, \langle \ln K_I \rangle) = 0$.

$\text{Cov}(n, \ln v_0)$ can now be evaluated by substituting equation (B1) for $\ln v_0$

$$\text{Cov}(n, \ln v_0) = \text{Cov}(n, \langle \ln v \rangle - n[\langle \ln K_I \rangle - \ln K_0]). \quad (B3)$$

But since n is not statistically dependent on $\langle \ln v \rangle$ or $\langle \ln K_I \rangle$,

$$\text{Cov}(n, \ln v_0) = -(\langle \ln K_I \rangle - \ln K_0) \text{Cov}(n, n), \quad (\text{B4})$$

and since $\text{Cov}(n, n) = V(n)$

$$\text{Cov}(n, \ln v_0) = -(\langle \ln K_I \rangle - \ln K_0) V(n) \quad (\text{B5})$$

which is the equation used in the text.

By similar arguments, it can be shown that for a Weibull analysis of strength data,

$$\begin{aligned} \text{Cov}(m, \ln \sigma_0) &= \text{Cov}(m, \langle \ln \sigma \rangle - \frac{1}{m} \langle \ln Q \rangle) \\ &= - \langle \ln Q \rangle \text{Cov}(m, 1/m) \\ &= \langle \ln Q \rangle V(m)/m^2 \end{aligned} \quad (\text{B6})$$



Table 1. Summary of Statistical Data - High Silica Glass

Crack Propagation Data

(with $K_0 = 1 \text{ Nm}^{-3/2}$)

Specimen	Data Points	n	$\ln v_0$
1	19	37.369	-498.68
2	19	34.400	-460.66
3	22	35.174	-470.09

$$\begin{aligned} \bar{n} &= 35.648; & V(\bar{n}) &= 0.791 \\ \overline{\ln v_0} &= -476.48; & V(\overline{\ln v_0}) &= 130.68 \\ \text{Cov}(\bar{n}, \overline{\ln v_0}) &= -10.165 \end{aligned}$$

Stress Intensity Factor Data (determined on 4 specimens)

$$\langle \ln K_{IC} \rangle = 13.454$$

$$V(\langle \ln K_{IC} \rangle) = 6.072 \times 10^{-4}$$

Strength Data

$$\begin{aligned} m &= 6.222 \text{ (determined on 30 specimens)} \\ V(m) &= 4.217 \times 10^{-2} \\ V(\epsilon) &= 3.9233 \times 10^{-2} \\ \langle \ln Q \rangle &= -0.5362 \end{aligned}$$

Table 2. Summary of Statistical Data

Hot Pressed Silicon Carbide

Crack Propagation Data

(with $K_0 = 1 \text{ Nm}^{-3/2}$)

n	=	23.6326
$V(n)$	=	0.7998
$V(\delta)$	=	9.8238×10^{-4}
$\langle \ln K_I \rangle$	=	14.528
N	=	21
$\ln v_0$	=	-353.67
$V(\ln v_0)$	=	168.83
$\text{Cov}(n, \ln v_0)$	=	-11.620

Stress Intensity Factor Data (determined on 8 specimens)

$\langle \ln K_{IC} \rangle$	=	15.146
$V(\langle \ln K_{IC} \rangle)$	=	9.2048×10^{-5}

Strength Data

m	=	9.401 (determined on 19 specimens)
$V(m)$	=	9.8439×10^{-2}
$V(\epsilon)$	=	2.3150×10^{-2}
$\langle \ln Q \rangle$	=	-0.5217

References

1. A.G. Evans and S.M. Wiederhorn, "Proof Testing of Ceramic Materials - An Analytical Basis for Failure Prediction," *Int. J. Fracture*, 10 [3], 379-392 (1974).
2. R.W. Davidge, J.R. McLaren and G. Tappin, "Strength-Probability-Time (SPT) Relationships in Ceramics," *J. Mater. Sci.*, 8, 1699-1705 (1973).
3. S.M. Wiederhorn, pp. 633-663 in *Ceramics for High Performance Applications*, eds. J.J. Burke, A.E. Gorum, and R.N. Katz, Brook Hill Publ. Co., Chestnut Hill, Mass. (1974).
4. B.J.S. Wilkins and L.A. Simpson, "Errors in Estimating the Minimum Time-to-Failure in Glass," *J. Am. Ceram. Soc.*, 57 [11], 505 (1974).
5. A.G. Evans, pp. 17-48 in *Fracture Mechanics of Ceramics*, Vol. 1, Eds. R.C. Bradt, D.P.H. Hasselman and F.F. Lange, Plenum Press, New York (1974).
6. S.M. Wiederhorn, pp. 613-646 in *Fracture Mechanics of Ceramics*, Vol. 2, Eds. R.C. Bradt, D.P.H. Hasselman, and F.F. Lange, Plenum Press, New York (1974).
7. J. Mandel, *The Statistical Analysis of Experimental Data*, Interscience, New York (1964).
8. J.S. Nadeau and J.N. Hay, "An Index of Resistance to Delayed Failure," *J. Can. Ceram. Soc.*, 43, 31-36 (1974).
9. O.L. Davies and P.L. Goldsmith, *Statistical Methods in Research and Production*, Harper Publ. Co., New York (1972).
10. W. Weibull, "A Statistical Theory of the Strength of Materials," *Ingeniörs Vetenskaps Akademien Handlingar*, No. 151, 1939.
11. B.L. Welch, "The Generalization of 'Student's' Problem When Several Different Population Variances are Involved," *Biometrika* 34, 28-35 (1947).
12. S.M. Wiederhorn, A.G. Evans, E.R. Fuller and H. Johnson, "Application of Fracture Mechanics to Space-Shuttle Windows," *J. Am. Ceram. Soc.* 57 [7], 319-323 (1974).
13. A.G. Evans and F.F. Lange, "Crack Propagation and Fracture in Silicon Carbide," *J. Mat. Sci.* in press.
14. J.R. Mathews, F.A. McClintock and W.J. Shack, "Statistical Determination of Flaw Density in Brittle Materials," *J. Am. Ceram. Soc.*, to be published.



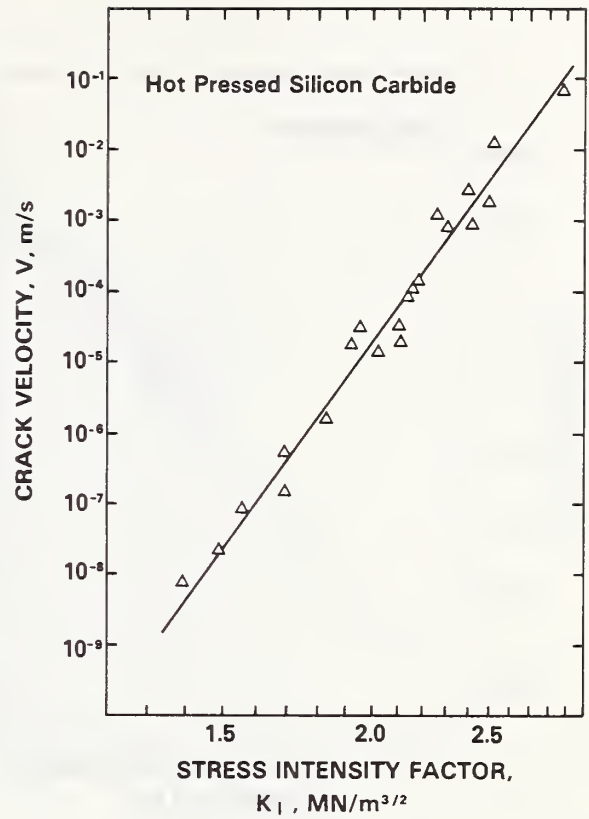
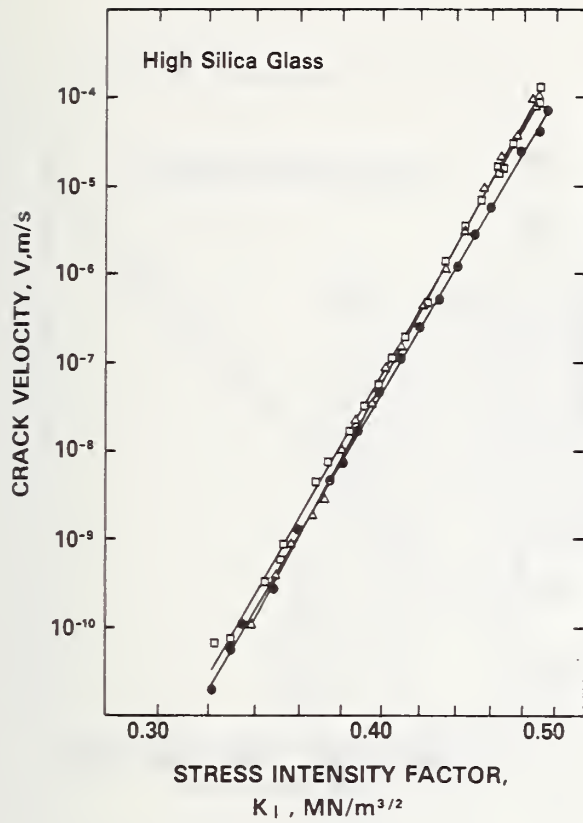


Figure 1. Crack velocity as a function of applied stress intensity factor
 (a) high silica glass tested in water
 (b) hot pressed silicon carbide tested in air at 1400°C.

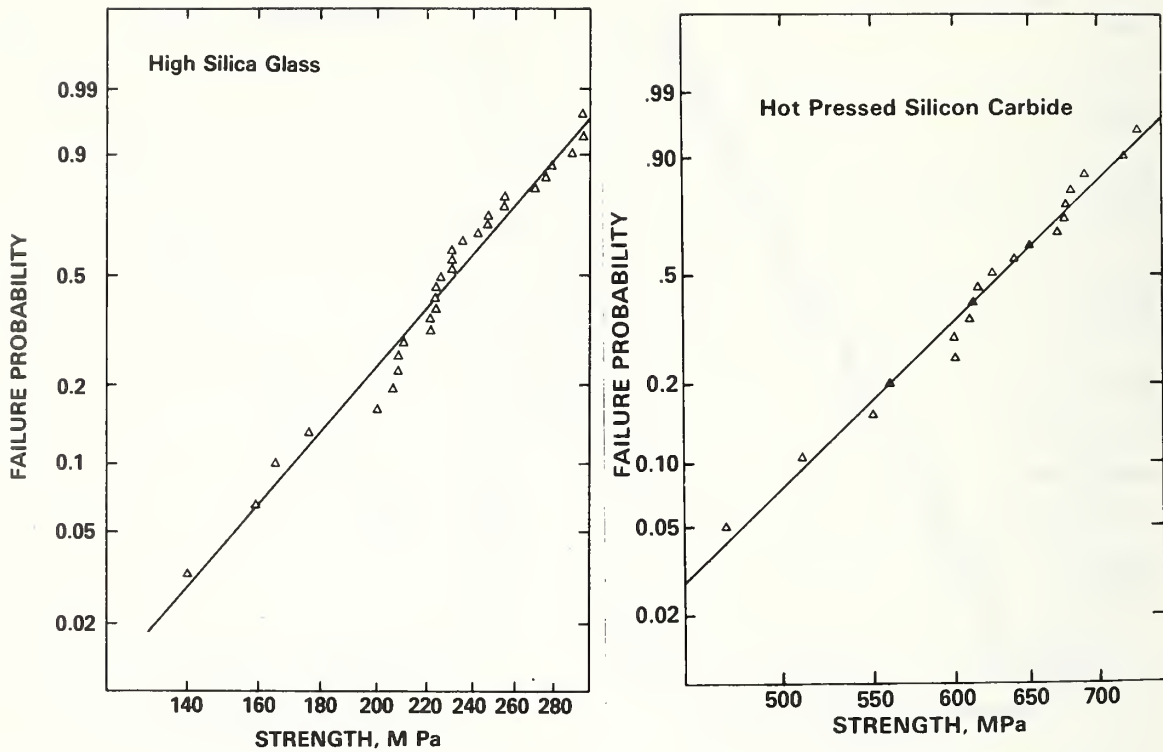


Figure 2. Strength as a function of cumulative failure probability, P ,
 (a) high silica glass tested in dry nitrogen
 (b) hot pressed silicon carbide tested in air at 25°C.

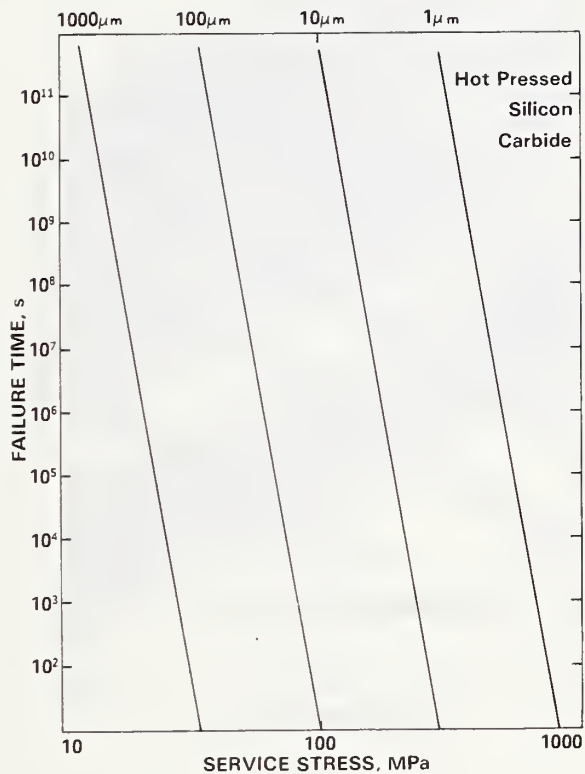


Figure 3. Design diagram based on direct flaw size measurement, silicon carbide. Size of flaws in this material, $\sim 100\mu\text{m}$, precludes their detection and analysis by statistical means, thus the lack of confidence bands on this diagram.

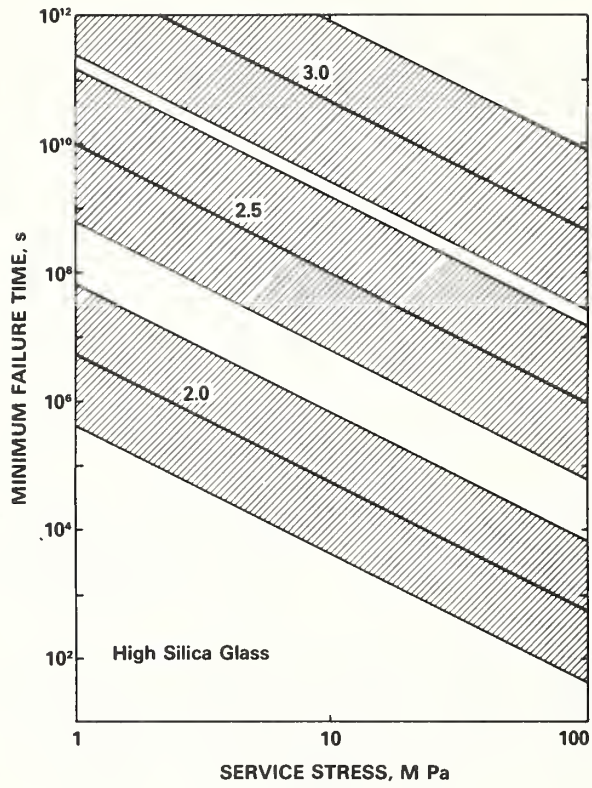


Figure 4. Design diagram based on proof testing, high silica glass.

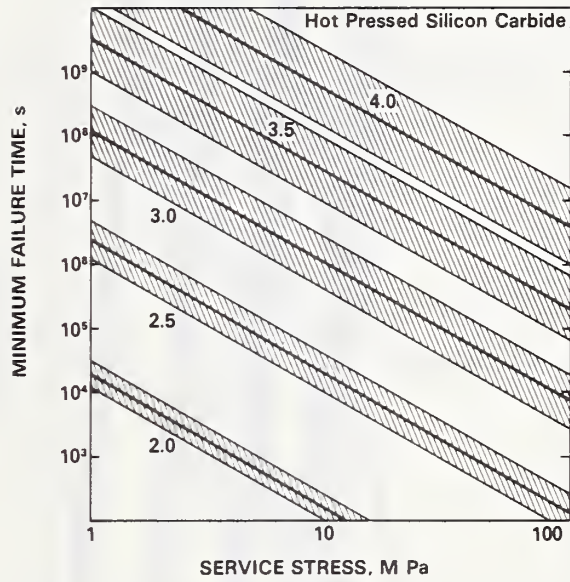


Figure 5. Design diagram based on proof testing, hot pressed silicon carbide.

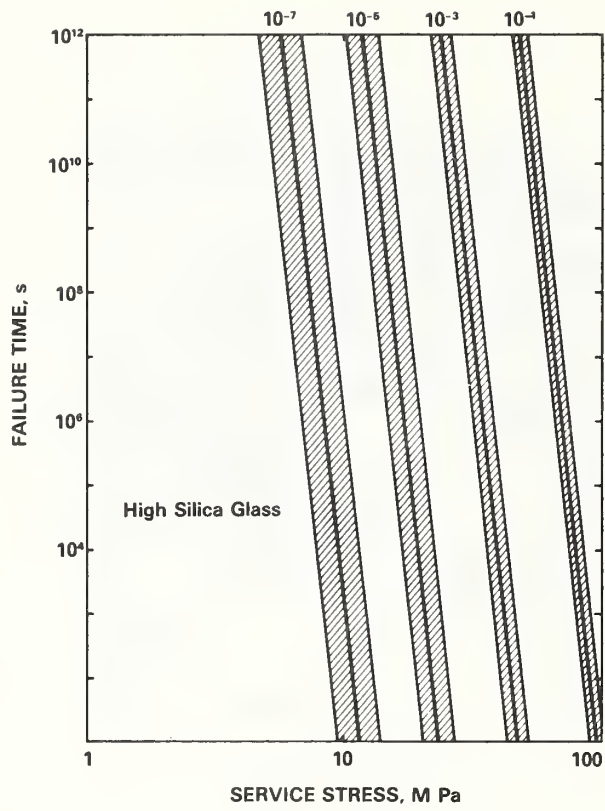


Figure 6. Design diagram based on strength measurements, high silica glass.

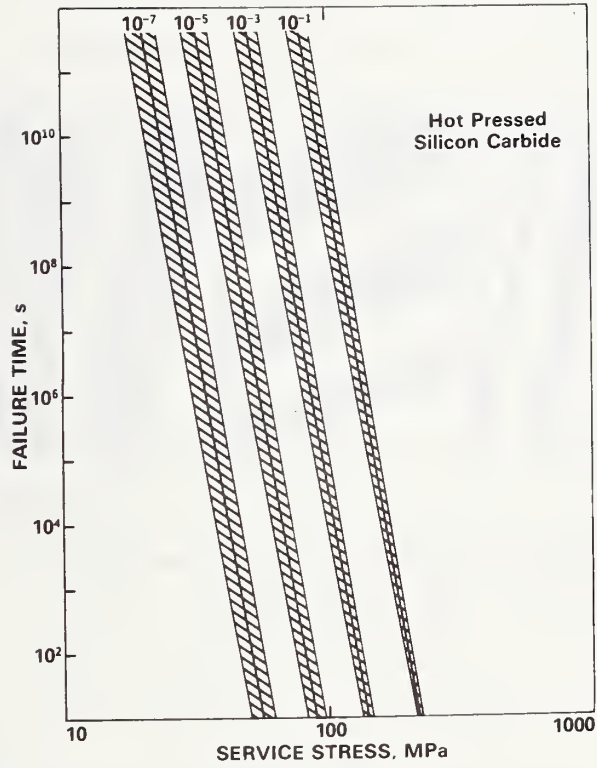


Figure 7. Design diagram based on strength measurements, hot pressed silicon carbide.

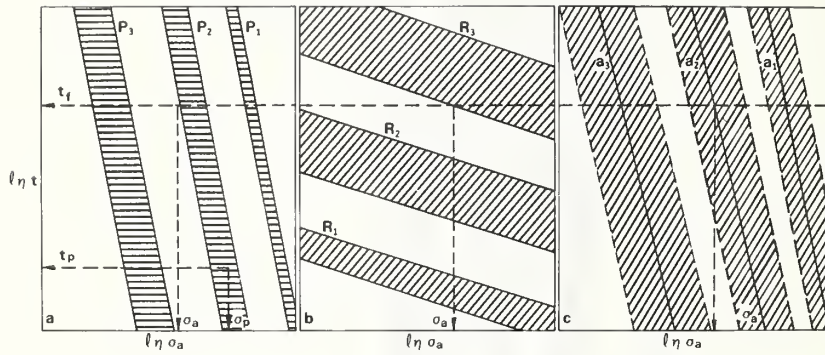


Figure 8. Composite design diagram.

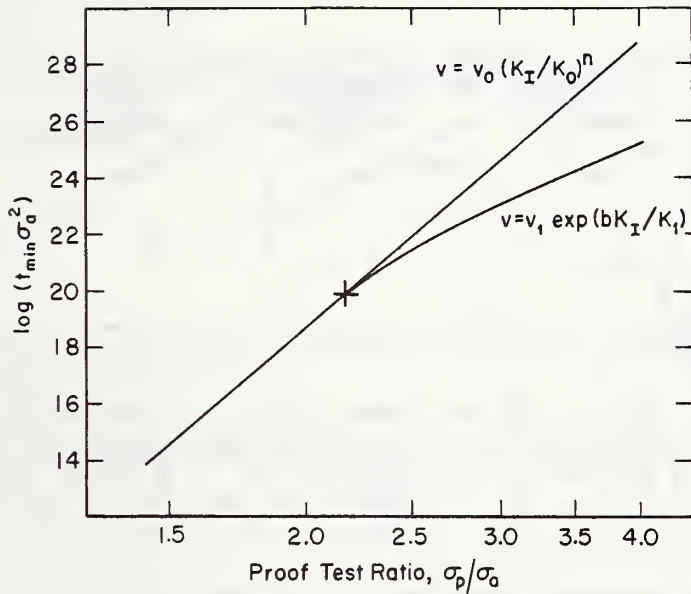


Figure 9. Proof test diagram comparing power function and exponential function representations of crack propagation data, high silica glass. The plus sign, +, in the figure marks the lower limit of the crack propagation data, reference 12.

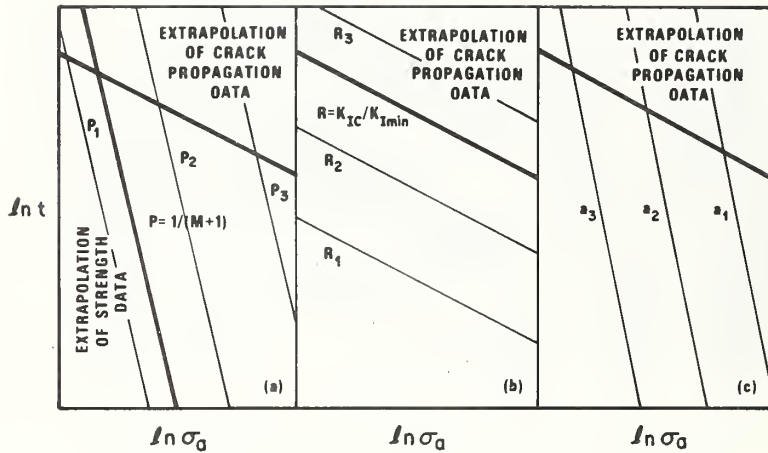


Figure 10. Schematic representation of design diagrams indicating regions of strength and crack propagation data extrapolation (a) strength method, contains two regions of extrapolation: one due to strength data; the other due to crack propagation data, (b) proof test method, (c) direct flaw measurement.

U.S. DEPT. OF COMM. BIBLIOGRAPHIC DATA SHEET	1. PUBLICATION OR REPORT NO. NBSIR 75-952	2. Gov't Accession No.	3. Recipient's Accession No.
4. TITLE AND SUBTITLE An Error Analysis of Failure Prediction Techniques Derived from Fracture Mechanics		5. Publication Date	6. Performing Organization Code
7. AUTHOR(S) S. M. Wiederhorn, E. R. Fuller, Jr., J. Mandel and A. G. Evans	8. Performing Organ. Report No.		10. Project/Task/Work Unit No.
9. PERFORMING ORGANIZATION NAME AND ADDRESS NATIONAL BUREAU OF STANDARDS DEPARTMENT OF COMMERCE WASHINGTON, D.C. 20234		11. Contract/Grant No. 3130459	
12. Sponsoring Organization Name and Complete Address (Street, City, State, ZIP) Air Force Materials Lab		13. Type of Report & Period Covered	14. Sponsoring Agency Code
15. SUPPLEMENTARY NOTES			
16. ABSTRACT (A 200-word or less factual summary of most significant information. If document includes a significant bibliography or literature survey, mention it here.) Three principal methods of failure prediction for brittle materials are analyzed statistically. Each method depends on fracture mechanics for its predictive value and hence, the variance of the failure time is found to depend on the scatter in the fracture mechanics data and the scatter in the estimate of the initial size of the strength limiting crack. The variance is used to calculate confidence limits for the prediction of failure for two materials, glass and silicon carbide. Procedures for the collection and analysis of data are discussed, and the implications of the analysis for lifetime prediction are evaluated.			
17. KEY WORDS (six to twelve entries; alphabetical order; capitalize only the first letter of the first key word unless a proper name; separated by semicolons) Crack propagation; error analysis; failure prediction; failure prevention; fracture; statistics; strength			
18. AVAILABILITY <input checked="" type="checkbox"/> Unlimited <input type="checkbox"/> For Official Distribution. Do Not Release to NTIS <input type="checkbox"/> Order From Sup. of Doc., U.S. Government Printing Office Washington, D.C. 20402, SD Cat. No. C13 <input checked="" type="checkbox"/> Order From National Technical Information Service (NTIS) Springfield, Virginia 22151		19. SECURITY CLASS (THIS REPORT) UNCLASSIFIED	21. NO. OF PAGES 40
		20. SECURITY CLASS (THIS PAGE) UNCLASSIFIED	22. Price \$4.00



